H-bond symmetrization in high pressure methane hydrate

Sofiane Schaack, Philippe Depondt, Fabio R.D. Finocchi

H-bond symmetrization in high pressure methane hydrate

IOP Conf. Series: Journal of Physics: Conf. Series **1136** (2018) 012018 doi:10.1088/1742-6596/1136/1/012018

H-bond symmetrization in high pressure methane hydrate

Sofiane Schaack[1], **Philippe Depondt**[1], **Fabio Finocchi**[1]

[1]Sorbonne Université, CNRS UMR 7588, Institut des Nanosciences de Paris ,INSP, 75005 Paris, France

E-mail: schaack@insp.jussieu.fr

Abstract. First-principle molecular dynamics simulations of methane hydrate MH-III, including the quantum properties of the hydrogen nuclei, were carried out at pressures in the 5-65 GPa range, in order to observe the H-bond symmetrization at high pressure and at room temperature. According to our simulations, the symmetrization transition takes place around 40 GPa and is little dependent on isotope substitution. We find that, consistently with the rather complex crystal structure of MH-III, the transition is much more convoluted in the hydrate than in ices VII and X. In methane hydrate, due to the presence of non equivalent O ions with distinct O-O distances, the dissimilar H bonds symmetrize in a pressure domain rather than at a single critical pressure.

1. Introduction

Methane hydrate (MH) is a clathrate compound in which methane molecules are trapped within a solid cage of water[1, 2]. MH could have occurred in the nebula from which ice giants Uranus and Neptune were formed and is still present on Titan [3, 4]. Significant deposits of methane clathrate hydrates have been also found on Earth, in cold upper sediments on the sea and ocean floors, which could be destabilized as the oceans warm up and release large quantities of greenhouse methane gas [5]. The previous facts motivated many researches on the stability of methane hydrates under various conditions.

The interaction between the host molecules and the cage is essentially repulsive; this is why methane hydrates were initially thought to be stable only at relatively modest pressure, below a few GPa. However, quite recently [6, 7], several phases of MH, differing by structure and composition, were found to be stable at very high pressures, beyond 10 GPa and up to ~ 100 GPa. At those pressures, not only could the interaction between the cage and the methane molecules be significantly altered as ice cages shrink, but the ice cage itself could undergo deep modifications. Indeed, the hydrogen bonds between the water molecules that form the cage may become symmetric and the ice cage eventually evolves towards a non-molecular form, which modifies the mechanical properties of the hydrate, as well as the molecule-cage interaction.

The hydrogen bond symmetrization under pressure was first observed in ice phase X. Along the transition from phase VII (H-bonds, with proton disorder) to phase X (symmetric bonds, proton ordered) the quantum properties of the hydrogen nuclei play an important role [8, 9]; the most striking one regards the computed transition pressure at room temperature, which is reduced from approximately 100 GPa within the classical frame down to 65 GPa, in agreement

with the experimental findings, when nuclear quantum effects are included. Among the latter, the zero-point energy (ZPE) is crucial in two respects: first, at the onset of proton tunneling between the two potential wells that correspond to the asymmetric H bond; second, in lowering the critical pressure for symmetrization with respect to the classical frame. In methane hydrate, a similar process is expected in the high-pressure MH-III phase, which is the stable phase of the system at ambient temperature and above 2GPa.

The paper is organized as follows: after a brief description of the simulation methods, in section 3 we first describe the order parameter that is commonly used to describe the H-bond symmetrization; then, we analyze the displacements of the proton along the O-O axis or normally to it (section 4); finally, we investigate the role of the interaction between the protons (deuterons) in the cage with the guest methane molecules in Section 5. All along the paper, we compare the behavior of the protons in MH-III to prototypical pure ice.

2. Computational details

Constant volume, constant temperature (NVT) molecular dynamics simulations at room temperature were carried out using the Quantum Thermal Bath method (QTB) [10] in order to include nuclear quantum effects. The QTB method is implemented in the Quantum Espresso [11] package. It is based on a Langevin equation in which the random force $R(t)$ is tailored to fulfill the quantum fluctuation-dissipation theorem [12]: instead of a white noise, one uses a colored noise with the following power spectrum:

$$\left|\tilde{R}(\omega)\right|^2 = 2m\gamma\hbar\omega \left[\frac{1}{2} + \frac{1}{\exp\left(\frac{\hbar\omega}{k_B T}\right) - 1}\right] \tag{1}$$

where m is the nucleus mass, k_B the Boltzmann's constant, T the temperature, $\omega/2\pi$ the frequency, and γ is the friction coefficient entering also the dissipation term in the Langevin equation. QTB is strictly exact only for harmonic systems. While dealing with anharmonicity, semi-classical methods such as QTB are submitted to zero-point energy leakage (ZPEL) which tends to equilibrate the energy distribution following the classical equipartition theorem. Adjusting the friction coefficient γ (eq 1) allows to lower the effect of the ZPEL [13] as the larger γ is the more the classical system is coupled to the quantum bath. Despite the widening of the vibrational peaks, the QTB has proven valuable in several systems [9, 14, 15, 16] and the QTB simulations presenting ZPEL have shown that they provide correct mode frequencies [17]. Rather importantly in the present context, a systematic comparison with the classical case can be carried out by simply replacing the colored QTB noise in equation (1) with the standard white noise $\left|\tilde{R}(\omega)\right|^2 = 2m\gamma\ k_B\ T$, while all the other computational ingredients remain identical [18].

The initial structure was taken from ref. [7]. The simulated samples consist of 16 methane molecules and 32 water molecules in a $2 \times 1 \times 2$ orthorhombic supercell. The methane molecules are hydrogenated (CH_4) while the ice cage is considered with hydrogenated (H_2O) or deuterated (D_2O) water molecules. The electronic structure and atomic forces were obtained within the Generalized Gradient approximation (GGA) [19] to the DFT. Van der Waals interactions were added by following the semi-empirical scheme by Grimme [20]; after extensive tests, a better agreement with experimental lattice constants and compressibility could be obtained with respect to the pure GGA. Ultra-soft pseudo-potentials were used to describe the interaction between the ionic cores and the valence electrons: a plane wave expansion cutoff of $E_{cut} = 40$ Ry ensures total energy and atomic force convergence. The friction coefficient was set to $\gamma = 1$ THz limiting the impact of ZPEL effects in the simulations which tend to underestimate NQE. Their impact was estimated to be at maximum $\sim 7\%$ of the temperature of the different degrees

of freedom of MHIII. Simulations were run at constant volume, with lattice parameters chosen to sample pressures from 5 up to 65 GPa by obtaining an isotropic stress tensor within our statistical error. Oxygen and carbon atoms were initially set at their crystallographic positions, while cage hydrogen atoms were let to relax during short simulations with large friction coefficients γ in order to explore different configurations and start with variable orientations for the CH_4 molecules. All atoms are free to move during the simulations. The typical duration time of the simulations is 30 ps.

3. Characterizing the symmetrization transition

Along the VII-X transition of ice under pressure, the effective potential that is felt by the proton in hydrogen bonds is usually described in terms of a one-dimensional double-well potential, along the O-O axis [21, 22]. As pressure increases, the oxygen-oxygen nearest neighbor separation continuously decreases: the distance between the double wells and the barrier is accordingly reduced, making it possible for the proton to tunnel back and forth between the two wells. Upon further contraction of the O-O distance, the proton has its largest probability halfway between the two O ions. The simplest order parameter and the most widely used[8, 9, 14, 16] to estimate the location of a hydrogen nucleus between the two nearest oxygen atoms is:

$$\chi = d(\mathrm{O}^{[1]} - \mathrm{H}) - d(\mathrm{O}^{[2]} - \mathrm{H}) \tag{2}$$

where $d(\mathrm{O}^{[n]} - \mathrm{H})$ is the distance between the selected proton and its n^{th} oxygen nearest neighbor. So defined, this parameter equals zero for proton-symmetric hydrogen bonds.

The order parameter χ was observed to depend on the $\mathrm{O}^{[1]}$-$\mathrm{O}^{[2]}$ distance $d(\mathrm{O}^{[1]} - \mathrm{O}^{[2]})$ in several H-bonded systems: below a threshold ($d(\mathrm{O}^{[1]} - \mathrm{O}^{[2]}) \simeq 2.42$Å), the probability density $P(\chi)$ is maximum at $\chi = 0$ and the H-bond becomes symmetric [22, 21]. As the O-O distances in MH-III are shorter than in ice VII at all pressures, it is reasonable to expect the symmetrization transition to happen at a lower pressure than the ice VII $\rightarrow$ X transition. Although direct measurements of the symmetrization of the hydrogen bonds in MH-III are still lacking, recent X-ray diffraction and Raman spectroscopy experiments [23, 24, 25] indicate a phase transition from MH-III to an High Pressure (HP) phase between 40 and 55 GPa although a precise description of the transition was not provided.

We show in figure 1 the probability distributions of the order parameter χ, averaged over all O-H..O bonds (top panel), and for each different OO distance (bottom panel), in MH-III as computed from our simulations. $P(\chi)$ evolves from a distribution with two maxima, which is characteristic of asymmetric hydrogen bonds, to a single-peak distribution, which denotes the symmetric hydrogen bonds, around 40 GPa. This points towards a symmetrization transition of the ice cage in MH-III around 40 GPa, therefore at a much lower pressure than in pure ice. One can also note that even at a quite low pressure the distribution does not vanish for $\chi = 0$ ($P(\chi = 0) \neq 0$) showing that the ice skeleton is proton disordered even at P $\sim$ 10 GPa.

However, the situation is more complex in MH-III than in pure ice: first, $P(\chi)$ behaves rather similarly in both hydrogenated and deuterated cages. This would imply that isotope effects are practically negligible, and that nuclear quantum effects are not very relevant, in striking contrast with the case of ice VII $\rightarrow$ X transition [22, 9, 6]. Second, there are three non equivalent O-O distances in MH-III (2.811, 2.807 and 2.783 Å detailed in figure 2a) as experimentally measured at 3 GPa [6]. The mean O-O distances along the dynamics can indeed be collected in three distinct groups, two of which ((a), corresponding to O1-O1$'$ and oriented along c; (b), connecting O1 to O6 in the notation of ref. [3]) have the same mean value $\bar{d}(\mathrm{O}^{[1]} - \mathrm{O}^{[2]})$ while the third group (c, corresponding to O1-O2 and O1-O2+, at the vertex of the 6-fold water rings) shows a slightly smaller mean O-O distance at all pressures. The corresponding probability distributions for the order parameter $P^{(\alpha)}(\chi)$, $\alpha = a$, b or c are sketched in the lower panels of figure 1. $P^{(\alpha)}(\chi)$, for $\alpha = a$ and b, shows two maxima at 40.6 GPa and 43.4 GPa for the

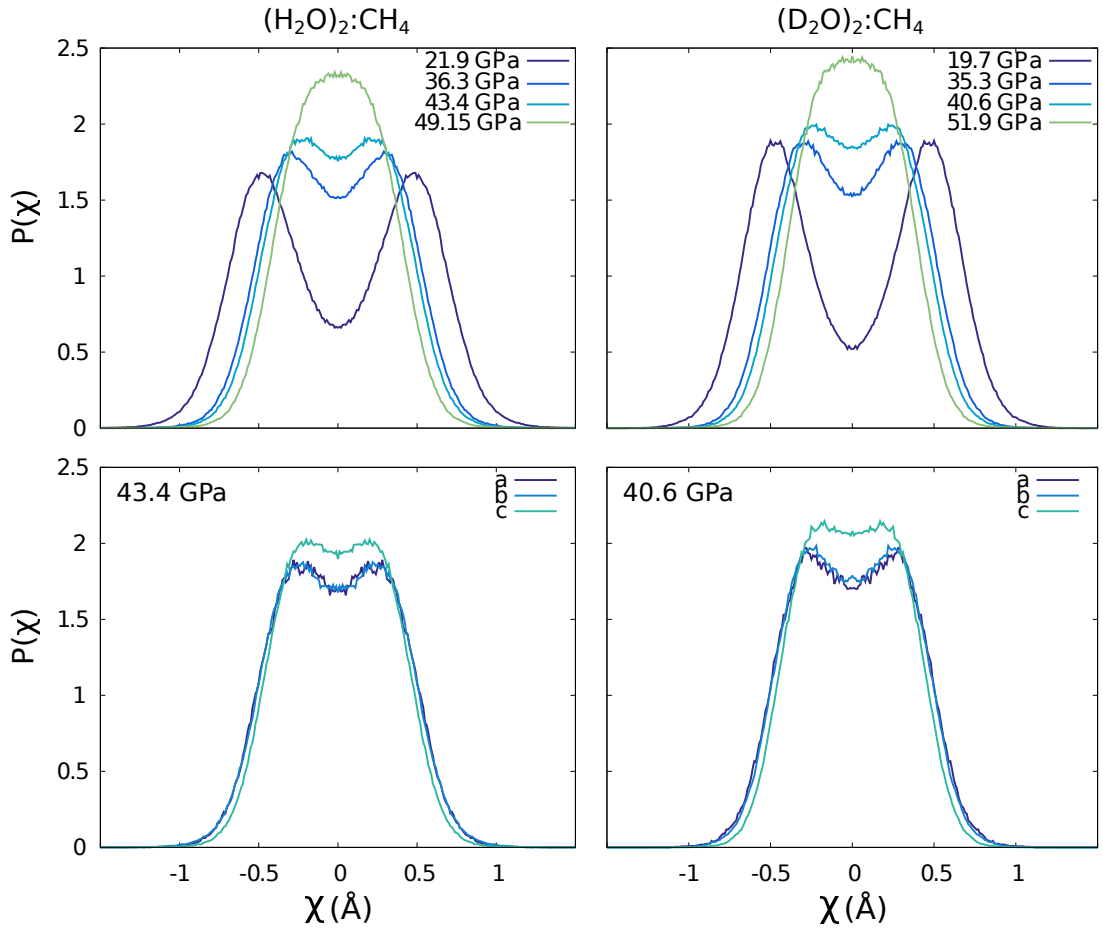

Figure 1. Distributions of the order parameter $P(\chi)$ at several pressures, for the hydrogenated (left) and deuterated (right) ice skeleton. Upper panels: $P(\chi)$ is computed by integrating on all hydrogen bonds. Bottom panels: Distributions of the order parameter $P(\chi)$ for each group of O-O equivalent distances (a, b, c) (see text).

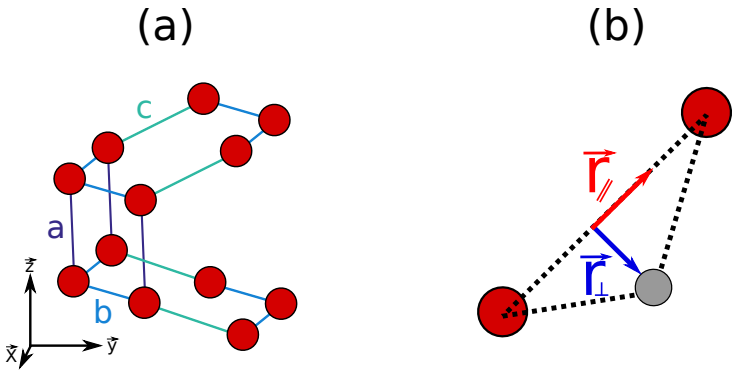

Figure 2. (a) The three different OO distances with $a \geq b > c$. (b) Description of the parallel $r_{\parallel}$ and normal $r_{\perp}$ proton delocalisation.

deuterated and hydrogenated ice skeletons, respectively, while $P^{(c)}(\chi)$ is flat around $\chi = 0$. The difference between the distributions reveals that the transition takes place in two steps:

at slightly lower pressures, the hydrogen bonds are symmetrized along the shorter O-O axes in group (c), and those in the remaining groups follow, with a delay corresponding to a few GPa. The picture that emerges from the $P^{(\alpha)}(\chi)$ distributions is that of a symmetrization transition that extends over ~ 5 GPa around 40 GPa rather than happening at a precise critical pressure, as in the case of pure ice [9].

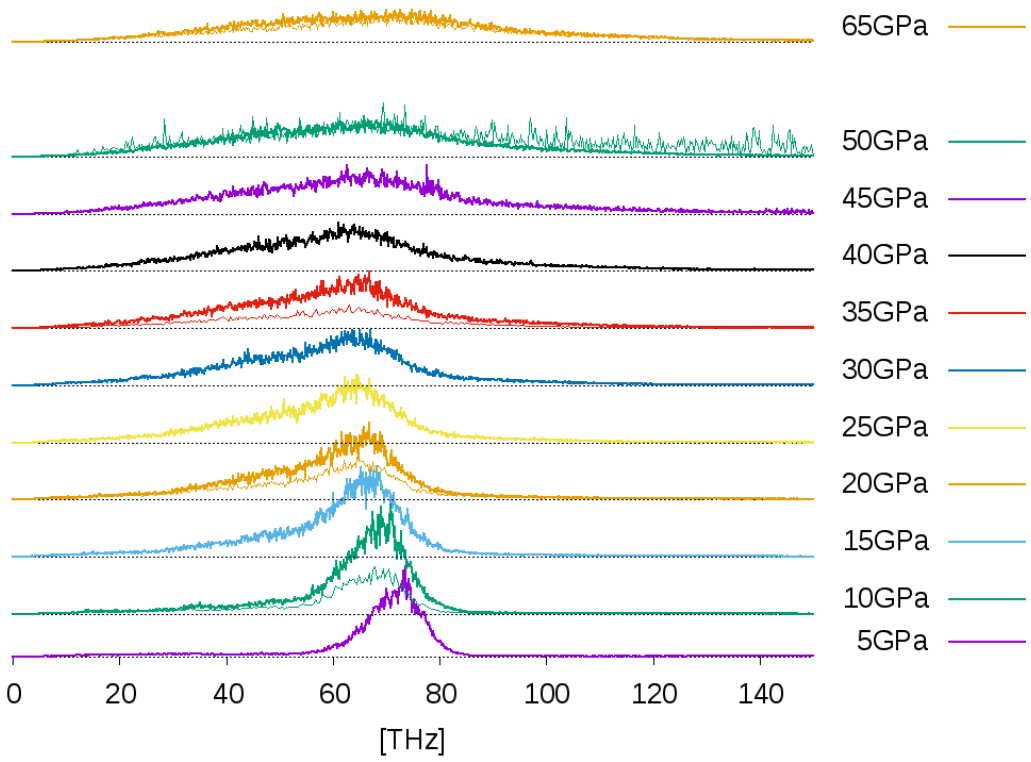

Figure 3. Fourier transforms in the frequency domain of the parallel component of the velocity-velocity time-correlation functions $\langle \dot{r}_{\parallel}(t)\dot{r}_{\parallel}(0)\rangle$ along the O-O axis. Thick line are for D_2O-CH_4, thin lines for H_2O-CH_4. The frequencies of the latter spectra were divided by $\sqrt{2}$ in order to take into account the mass difference.

In order to confirm the indications that we obtained from the trends of the order parameter χ, we computed the vibrational spectra through the Fourier transforms (FT) of the time correlation functions. In particular, we examined the velocity-velocity time correlation functions $\langle \dot{r}_{\alpha}(t)\dot{r}_{\alpha}(0)\rangle$, where r_{α} is the α component of vector joining the proton (deuterium) in the ice cage and its oxygen first neighbor $O^{[1]}-H$. We then considered the projections of the previous vectors parallel or perpendicular ($r_{\parallel}$ and $r_{\perp}$, respectively, detailed in Figure 2b) to the $O^{[1]}-O^{[2]}$ axis. The spectra of the parallel components $\dot{r}_{\parallel}$ show a shallow minimum of the mode's frequency around 35-40 GPa, which is consistent with the softening of the shorter H bonds (figure 3). Such a softening is a signature of the symmetrization transition, as discussed in the case of pure ice [9, 22], which points towards a critical pressure around 35-40 GPa, which is slightly smaller but consistent with the indications from the distribution of the corresponding order parameter χ. As for the $P(\chi)$ distributions, the spectra for hydrogenated and deuterated ice cages little differ once the latter have been renormalized by the mass ratio $\sqrt{2}$, confirming that nuclear quantum effects do not play a crucial role in the symmetrization transition of MH-III. As it downshifts, the OD stretching mode peak intensity flattens, thus the uncertainty on the mode's frequency

prevents the difference of $P(\chi)$ distributions in terms of the three OO distances (Figure 2a) to be resolved. The distinction between the proton motion along or normally to the O-O axis translates also in the distributions of the proton (deuterium) localization, which we analyze in the following.

4. Analysis of the proton delocalization

Using simulation data from [9], we compare the hydrogen distribution with that of ice under pressure in which the VII→X transition shows important nuclear quantum effects, in constrast with methane hydrate.

First, we show (figure 4) the hydrogen distribution for both ice and methane hydrate with the same scales and normalization, for comparison. One observes that the OH $r_{\parallel}$ distance is approximately the same in both compounds as are the parallel widths, while the perpendicular extension is larger for the hydrate at all pressures.

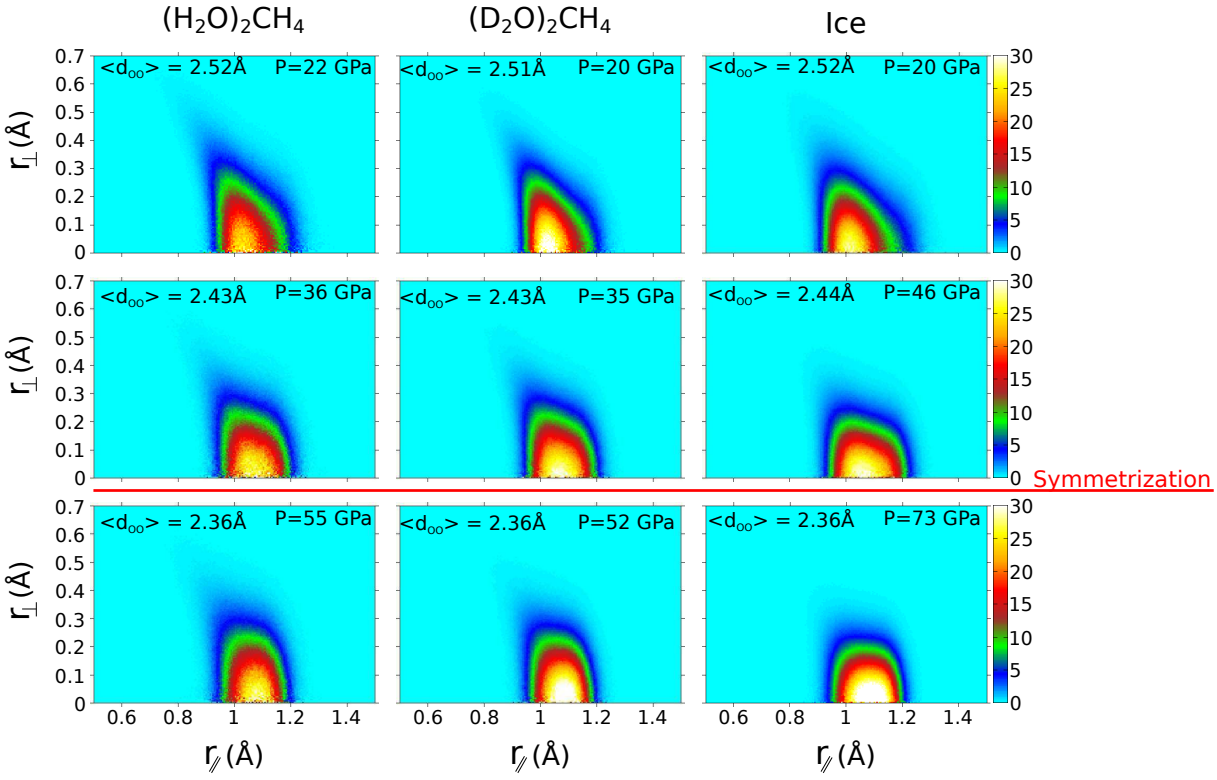

Figure 4. Probability density $P(r_{\parallel}, r_{\perp})$ for $(H_2O)_2 : CH_4$ (left) $(D_2O)_2 : CH_4$ (middle) and ice (right) systems at three pressures : one below the transition, one not very far from it and one above. Pressure values have been selected in order that the mean OO distances $< d_{oo} >$ in the three systems match, as the hydrogen bond symmetrization process is controlled by this parameter.

In order to obtain a more quantitative result one may compute the mean value of $r_{\parallel}$ and parallel $\sigma_{\parallel}$ and perpendicular $\sigma_{\perp}$ standard deviations (figure 5). This clearly confirms a broader distribution in the normal direction than along the O-O axis, and suggests that a purely one-dimensional model hamiltonian, like those usually adopted [22, 21] are unable to catch the complexity of the hydrogen bond in methane hydrate or other highly anisotropic systems. A finer analysis based on the differences of $P(r_{\parallel}, r_{\perp})$ between the hydrogenated and deuterated cages shows that the radial delocalization is larger in the case of $(H_2O)_2 : CH_4$. From the

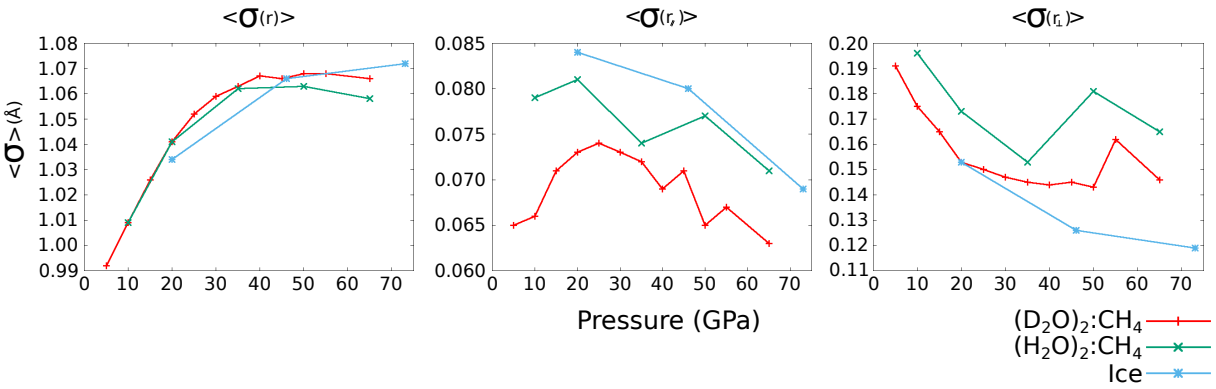

Figure 5. Ice and methane hydrate systems : (left) mean $r_{\|}$, (middle) parallel and (right) perpendicular standard deviations.

theoretical analysis of normal modes and accurate Raman measurements, it can be deduced that the interactions between the water cage and the methane molecules play a significant role in the system's dynamics, starting at a pressure of 20GPa [26]. Figure 4 shows the probability $P(r_{\|}, r_{\perp})$: the normal contributions to the distribution are broad with a significant amplitude up to $r_{\perp} \approx 0.4$ Å. The inverted comma shape of the distribution indicates that the hydrogen atoms, as they move about, tend to retain a relatively constant O-H distance. As pressure is increased, the shape of the distribution changes: the parallel contribution is sensitive to increased tunneling and thus broadens until approximately 40GPa while the normal contribution tends to shrink slightly.

5. Molecule-cage interaction

A step further in the analysis between the ice cage and the methane molecules is taken with the conditional probability $\rho(d_{\mathrm{HH}}|r_{\perp})$ (resp. $\rho(d_{\mathrm{DH}}|r_{\perp})$) which is computed for the cage hydrogen (deuterium) nuclei: d_{HH} (d_{DH} for deuterium) is the distance between a cage hydrogen nucleus and the closest hydrogen nucleus of a methane molecule. The point is now to assess how the interaction of the methane molecules with the cage acts upon the lateral motion of the cage hydrogen atoms. Figure 6 shows a clear correlation between the presence of a methane hydrogen and the sideways displacement of the cage hydrogen (deuterium) atoms for all examined pressures and without clear indication of a change at the alleged transition pressure of 40GPa. When protons in the CH_4 molecules approach the cage hydrogen (deuterium) below a typical distance ($\sim 2.0\mathring{A}$ at P=10 GPa, $\sim 1.9\mathring{A}$ at P=35 GPa and $\sim 1.7\mathring{A}$ at P=65 GPa), $r_{\perp}$ tends to increase, in order to maximize d_{HH} (resp. d_{DH}). This provides an insight into the reason why no clear isotopic effect can be seen at the transition pressure: we know that a small asymmetry in a double well potential can severely reduce tunneling between the two wells [14], now our results show that the effective double well in which the cage hydrogen nuclei reside is perturbed by the molecular hydrogen nuclei. This shows that the normal delocalization is a result of the repulsive interaction between the hydrogen (deuterium) in the cage and those in the methane molecule.

Other simulations were carried out, removing the methane molecules while keeping the oxygen atoms fixed to their original positions and letting the cage hydrogen atoms move freely: the result thereof is that these hydrogen atoms escape from the O-O axes, which shows that the repulsive interactions between the hydrogen of the host CH_4 molecules and the cage hydrogen (resp. deuterium) is also necessary for the stability of the H bonds in the latter frame. It seems that the effect of the environment on the O-H-O groups, due to the presence of the methane

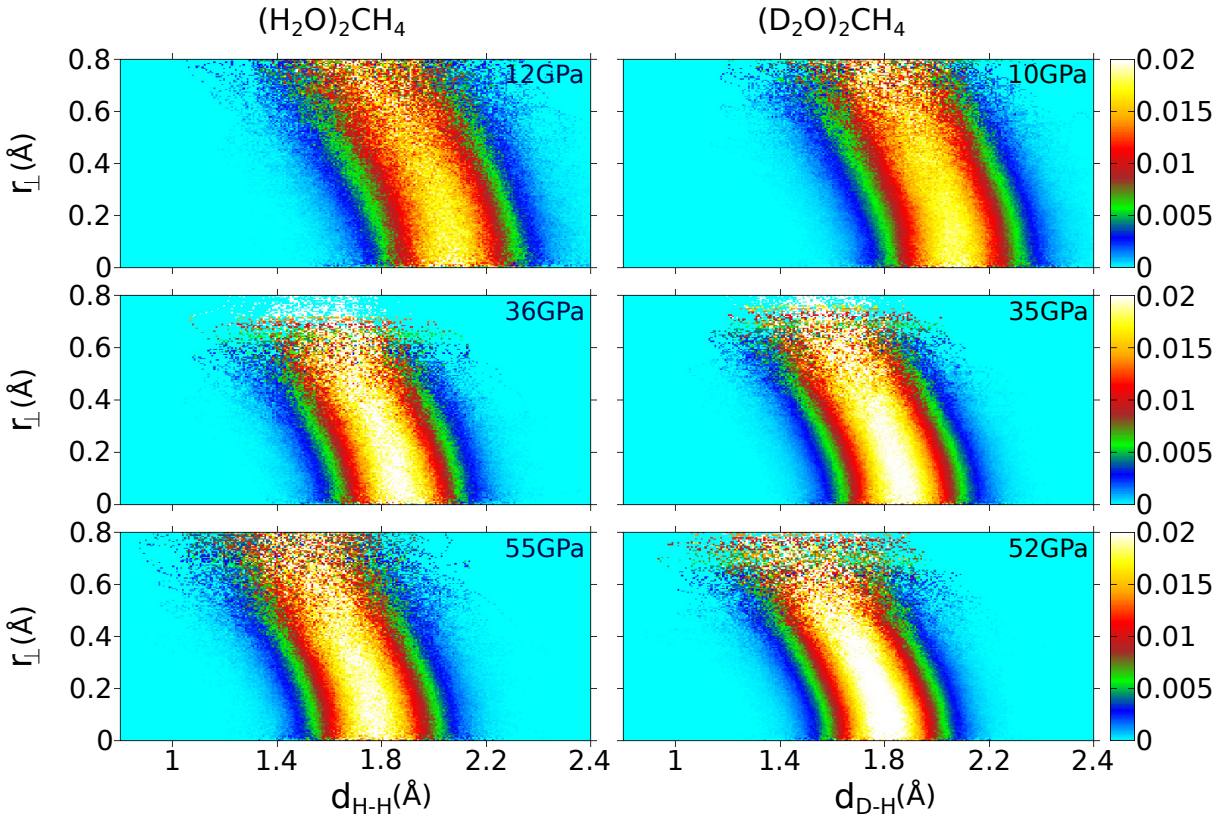

Figure 6. Conditional probability $\rho(d_{\mathrm{HH}}|r_{\perp})$ for a hydrogenated cage (left panels) or deuterated cage (right panels).

molecules is to keep the hydrogen atoms close enough to the straight line between the oxygen atoms, but not on it.

6. Concluding remarks

According to previous suggestions, we confirm that, assuming the MH-III structure remains stable at these pressures, a symmetrization transition should occur at approximately 35-40 GPa, much below that in ice VII→X transition due to the smaller O-O distances in methane hydrate with respect to pure ice at all pressures. Moreover, in MH-III, we observe two main groups of hydrogen bonds corresponding to distinct O-O distances, which symmetrize at slightly different pressures. This behaviour contrasts with that of the ice VII where all hydrogen bonds are equivalent and symmetrize at the same pressure. Appropriate spectral experiments could provide a confirmation thereof.

Another difference between ice and MH-III is the isotope effect. While in pure ice the H → D substitution significantly upshifts the symmetrization transition pressure, we found that the symmetrization of the hydrogen bonds occurs at almost same pressures in the hydrogenated and deuterated cages of methane hydrate. Both the lower symmetry of MH-III with respect to pure ice and the interaction between the confined methane molecules and the protons (deuterons) in the H bonds are at the root of a more complex behavior. In particular we observe in methane hydrate an increase of the lateral disorder of the cage hydrogen (deuterium) atoms, as compared with ice VII and X, which points towards a reduction of nuclear quantum effects. As a matter of fact, protons in MH-III cages are more delocalized than deuteriums in both longitudinal and normal directions along the O-O axis. Our results thus exhibit a rather complex and/or subtle

behavior of the cage hydrogen atoms close to the symmetrization transition and should hopefully constitute a strong enticement for experimental endeavours in the same pressure range.

6.1. Acknowledgments
We would like to thank L.E. Bove, U. Ranieri and R. Gaal for useful discussions. We acknowledge critical reading of the manuscript by Simon Huppert. This work was granted access to the HPC resources of CINES under the allocation A0010906719 made by GENCI.

References

[1] Sloan J E D and Koh C 2007 *Clathrate hydrates of natural gases* (CRC press)
[2] Demirbas A 2010 *Methane gas hydrate: as a natural gas source* (Springer)
[3] Loveday J, Nelmes R, Guthrie M, Belmonte S, Allan D, Klug D, Tse J and Handa Y 2001 *Nature* **410** 661–663
[4] Hirai H, Hasegawa M, Yagi T, Yamamoto Y, Nagashima K, Sakashita M, Aoki K and Kikegawa T 2000 *Chem. Phys. Lett.* **325** 490–498
[5] Mascarelli A 2009 *Nat. rep. Clim. Change* 46–49
[6] Loveday J, Nelmes R, Guthrie M, Klug D and Tse J 2001 *Phys. Rev. Lett.* **87** 215501
[7] Loveday J and Nelmes R 2008 *Phys. Chem. Chem. Phys.* **10** 937–950
[8] Benoit M, Marx D and Parrinello M 1998 *Nature* **392** 258
[9] Bronstein Y, Depondt P, Finocchi F and Saitta A M 2014 *Phys. Rev. B* **89** 214101
[10] Dammak H Chalopin Y L M H M G J J (2009) *Phys. Rev. Lett.* **103** 190601
[11] Giannozzi P, Baroni S, Bonini N, Calandra M, Car R, Cavazzoni C, Ceresoli D, Chiarotti G L, Cococcioni M, Dabo I and et al 2009 *J. Phys. Condens. Matter* **21** 395502
[12] Callen H B and Welton T A 1951 *Phys. Rev.* **83**(1) 34–40
[13] Brieuc F, Bronstein Y, Dammak H, Depondt P, Finocchi F and Hayoun M 2016 *J. Chem. Theory Comput.* **12** 5688–5697
[14] Bronstein Y, Depondt P, Bove L, Gaal R, Saitta A M and Finocchi F 2016 *Phys. Rev. B* **93** 024104
[15] Dammak H, Antoshchenkova E, Hayoun M and Finocchi F 2012 *J. Phys. Condens. Matter* **24** 435402
[16] Bronstein Y, Depondt P and Finocchi F 2017 *Eur. J. Mineral.* 1–11
[17] Calvo F, Van-Oanh N T, Parneix P and Falvo C 2012 *Phys. Chem. Chem. Phys.* **14** 10503–10506
[18] One can easily verify that the colored noise in equation 1 reduces to the classical white noise with an additional term $\frac{\hbar\omega}{2}$ accounting for the zero point energy when $\frac{\hbar\omega}{k_B T} \to 0$
[19] Perdew J P, Burke K and Ernzerhof M 1996 *Phys. Rev. Lett.* **77** 3865
[20] Grimme S 2006 *J. Comput. Chem.* **27** 1787–1799
[21] Lin L, Morrone J A and Car R 2011 *J. Stat. Phys.* **145** 365–384
[22] Schweizer K S and Stillinger F H 1984 *J. Chem. Phys.* **80** 1230–1240
[23] Machida S I, Hirai H, Kawamura T, Yamamoto Y and Yagi T 2006 *Phys. Earth Planet. Inter.* **155** 170–176
[24] Machida S I, Hirai H, Kawamura T, Yamamoto Y and Yagi T 2007 *Phys. Chem. Miner.* **34** 31–35
[25] Tanaka T, Hirai H, Matsuoka T, Ohishi Y, Yagi T, Ohtake M, Yamamoto Y, Nakano S and Irifune T 2013 *J. Chem. Phys.* **139** 104701
[26] Schaack S, Ranieri U, Depondt P, Gaal R, Kuhs W F, Falenty A, Gillet P, Finocchi F and Bove L E *To be published*